G Model
ANL 1827 1–6

ARTICLE IN PRESS

Auris Nasus Larynx xxx (2013) xxx–xxx

Contents lists available at ScienceDirect

Auris Nasus Larynx

journal homepage: www.elsevier.com/locate/anl

Effects of arginine vasopressin on auditory brainstem response and cochlear morphology in rats

Hideaki Naganuma [a,*], Katsumasa Kawahara [b], Koji Tokumasu [a], Ryohei Satoh [b], Makito Okamoto [a]

[a] Department of Otorhinolaryngology, Kitasato University School of Medicine, 1-15-1 Kitasato, Minami-ku, Sagamihara, Kanagawa 252-0374, Japan
[b] Department of Physiology, Kitasato University School of Medicine, 1-15-1 Kitasato, Minami-ku, Sagamihara, Kanagawa 252-0374, Japan

ARTICLE INFO

Article history:
Received 23 June 2013
Received in revised form 1 December 2013
Accepted 9 December 2013
Available online xxx

Keywords:
Meniere's disease
Endolymphatic hydrops
Arginine vasopressin
Intermediate cell
Stria vascularis
Vacuole

ABSTRACT

Objective: This study was conducted to evaluate the relationship between hearing and cochlear histopathology after arginine vasopressin administration in rats.
Methods: A total of 30 Wistar rats were injected with either 0.02 unit/g of arginine vasopressin or the same amount of isotonic saline solution. The initial auditory brain stem response threshold was recorded and additional measurements were made at 10, 30, 60, and 90 min after injection of arginine vasopressin or isotonic saline solution. The threshold for each timepoint was compared with the initial threshold. Histological quantitative assessment of endolymphatic hydrops in the cochlea was performed using light microscopy and assessment of the basal, intermediate, and marginal cells of the stria vascularis was performed with electron microscopy.
Results: The auditory brain stem threshold 60 min after arginine vasopressin injection increased significantly in comparison with the initial threshold ($P < 0.05$). Although the index for endolymphatic hydrops in rats administered arginine vasopressin was not different from that in controls ($P > 0.05$), vacuoles in the intermediate cells were increased significantly in the treated rats ($P < 0.01$).
Conclusion: Hearing impairment was detected without endolymphatic hydrops in rats administered arginine vasopressin. An increase of vacuoles in the intermediate cells may account for the hearing impairment induced by arginine vasopressin injection.

Introduction

Endolymphatic hydrops, a histopathological finding in the inner ear of patients with Meniere's disease, is caused by morphological changes in the labyrinth brought about by an imbalance of water and ion metabolism. This disorder is characterized by a bulge in Reissner's membrane due to enlargement of the scala media space [1,2]. The mechanisms responsible for the development of this condition remained to be clearly understood.

A number of clinical and experimental studies have suggested that arginine vasopressin (AVP) may be involved in the development of endolymphatic hydrops [3–9]. Researchers have reported that administration of a large amount of AVP can induce endolymphatic hydrops in guinea pigs [5,7]. These studies revealed dilatation of the scala media associated with extension of Reissner's membrane toward the scala vestibuli in histological sections. It is well known that secretion of intrinsic AVP increases with high serum osmotic pressure and/or with a decrease in circulatory blood volume to prevent loss of water and mineral ions from the body. Physical or mental stress also becomes a factor involved in increased secretion of intrinsic AVP [10].

In previous reports detailing the development of endolymphatic hydrops in guinea pigs, the question remained as to whether or not AVP administration could lead to hearing impairment. Thus, our study was planned to explore the relationship between hearing and both light and electron microscopic findings in the inner ear after AVP administration in rats.

Materials and methods

This study was approved by Kitasato University School of Medicine, Animal Care and Use Committee. This study was approved by Kitasato University School of Medicine, Animal Care and Use Committee. A total of 30 male 5-week-old Wistar rats weighing 100–200 g were used. After administration of AVP or isotonic saline solution the following three evaluations were performed: (1) recordings of auditory brainstem responses (ABR) to reveal hearing impairments, (2) histological study of the inner

* Corresponding author. Tel.: +81 42 778 8432; fax: +81 42 778 8441.
E-mail addresses: naganuma@kitasato-u.ac.jp (H. Naganuma), kawahara@nc.kitasato-u.ac.jp (K. Kawahara), cjb14540@ams.odn.ne.jp (K. Tokumasu), ryou@kitasato-u.ac.jp (R. Satoh), okamotom@med.kitasato-u.ac.jp (M. Okamoto).

0385-8146/$ – see front matter © 2013 Published by Elsevier Ireland Ltd.
http://dx.doi.org/10.1016/j.anl.2013.12.004

ear by light microscopy to evaluate development of endolymphatic hydrops, and (3) electron microscopy (EM) of the stria vascularis to quantify the cytoplasmic vacuoles. Both side of ear in each rat were used for the evaluations.

Hearing impairment evaluation

The initial ABR threshold was recorded, after which 0.02 unit/g of AVP (Pitressin; Arg-vasopressin, Daiichi-Sankyo, Japan) was injected intraperitoneally to five rats and the same volume of isotonic saline solution injected to five control rats. The ABR threshold was measured at 10, 30, 60, and 90 min after the injection. The interval time between the two latencies of the first and third peak-wave of ABR was measured at each timepoint.

Measurements were made in a soundproof room. Rats were anesthetized with intraperitoneal pentobarbital sodium (35 mg/kg). Two silver-coated screws, 1 mm in diameter, were inserted on the midline of the vertex (one on the forehead as a negative and the other as a positive electrode). A ground electrode was inserted subcutaneously into the back. Click sounds of 0.1-ms duration were given for each ear through a speculum connected to a headphone at a rate of 10 Hz. A total of 512 responses were band-pass filtered at 50–3000 Hz and averaged with a Neuropack Sigma system (Nihon Koden, Tokyo, Japan).

ABR thresholds were determined by visual detection of reproducible responses, with a descending series of click intensities in 10-dB sound pressure level (SPL) steps. We regarded a reproducible response observed within 10 ms after a click presentation as positive, and the smallest intensity of clicks that evoked a visually detectable response of the first peak as the threshold. All responses were double traced to confirm their reliability.

Histological study of the inner ear

AVP at a dose of 0.02 unit/g or the same volume of isotonic saline was administered to rats in AVP group (five rats) or control group (five rats), respectively. One hour after the injection rats were transcardially perfused with isotonic saline while deeply anesthetized with pentobarbital sodium. Fixation was performed with 4% paraformaldehyde. The temporal bone was removed and further fixed in 4% paraformaldehyde in a cold room at 4 °C for ≥10 days. Thereafter, specimens were decalcified with 10% ethylenediaminetetraacetic acid (EDTA) for 3 weeks, dehydrated in a graded ethanol series, and embedded in Technovit 7100 (Heraeus Kulzer GmbH & Co. KG, Wehrheim, Germany). Blocks were cut horizontally into 10-μm sections, stained with hematoxylin and eosin, and observed under a light microscope (Olympus Provis AX80, Tokyo, Japan).

For quantitative assessment of morphological changes in the endolymphatic space, ratios of the length (Ir-L) of Reissner's membrane and a cross-sectional area of the scala media (Ir-S) were measured from the mid-modiolar section of the cochlea. The measurements and evaluation were performed as previously described [6], with some improvements. The temporal bones were decalcified with 10% EDTA instead of 5% trichloroacetic acid, and embedded in Technovit 7100 instead of paraffin–celloidin mixture. These changes may have improved the evaluation of the Ir-L and Ir-S ratio because the shrinkage ratio of tissues using the new agents was smaller than that previously reported. Ashlar-Vellum 3D (Ashlar, Austin, TX, USA) measuring software was used for the analysis and both ears from each rat were assessed.

EM of the stria vascularis

One hour after the injection of 0.02 unit/g of AVP or the same volume of isotonic saline solution, five rats from each group were euthanized and their temporal bones removed. Two small holes were made on the lateral bony wall, one on the cochlea area of the apical turn and the other on the vestibular organ. The cochleae in the bilateral inner ears were then fixed by perilymphatic perfusion of fixative containing 2.5% glutaraldehyde in 0.1 M phosphate buffer (pH 7.2) via the hole on the wall of the vestibular organ. The precise time between euthanasia and tissue fixation was measured to ensure fixation quality and enable reliable comparisons.

Each extirpated cochlea was immersed in the same fixative for 2 h at 4 °C. The tissue samples were washed in 7% sucrose in 0.1 M phosphate buffer (pH 7.2) at 4 °C overnight. Then, they decalcified with 10% EDTA for 5 weeks, trimmed at the columella cochlea plane, and fixed with 2% buffered osmium tetroxide for 2 h. After fixation, the tissue was washed in 0.1 M phosphate buffer (pH 7.2), dehydrated in a graded ethanol series, and embedded in Quetol 651 resin mixture (Nissin EM Co., Tokyo, Japan). Ultrathin sections were stained with 3.5% uranyl acetate for 25 min and lead citrate for 5 min, and then observed under transmission EM (TEM; JEM-1230; JEOL Ltd., Tokyo, Japan) at 80 kV.

The stria vascularis facing the tympanic cavity at the second turn in the mid-modiolar section of the cochlea was selected for assessment because the second turn was the most stable during histological section preparation, because the apical and basal turns may have been damaged by the holes made for perilymphatic perfusion. For qualitative analysis, the whole stria vascularis was observed. As there was enlargement of an area lacking intracellular organelles in the intermediate cells or a so called "vacuole" was observed, it was quantitatively assessed. In the intermediate cells, vacuoles of various sizes existed. Microvacuoles with a diameter <1 μm were indistinguishable from the normal space between the intracellular organelles. Therefore, in the present study, "vacuole" was defined as a nonstructural area with a diameter ≥1 μm. Attempts were made to quantitatively evaluate the difference in the total amount of defined "vacuoles" in the intermediate cells in the whole of the stria vascularis between the control and AVP groups. The stria vascularis was photographed at 2000× magnification using TEM, scanned at 400 dpi, and saved in a computer. The images were then merged with Adobe Photoshop Element 3.0 software (Adobe Systems Incorporated, Mountain View, CA, USA) and the entire stria vascularis saved as 1 image (Fig. 3A and B). The total area of each defined "vacuole" in the intermediate cells was measured in the whole of the stria vascularis with National Institute of Health (NIH) Image J ver. 1.44 software (http://rsb.info.nih.gov/ij/index.html).

To account for size disparity of each stria vascularis, the total area of defined "vacuoles" and the stria vascularis were measured in the same way and the ratios of the former to the latter calculated and compared between the control and AVP groups. The portion of the stria vascularis hidden behind the bar of the grid mesh (EM fine grid, F-150 mesh, Nissin EM Co.) for TEM was excluded from the calculations (Fig. 3A). The absence of defined "vacuoles" in marginal and basal cells was also confirmed.

Statistical analyses

A Mann–Whitney *U*-test or Wilcoxon signed-rank test was applied to find the difference between two independent or paired groups. To detect significance among ABR thresholds of a series of timepoints, a Friedman test was used to obtain a global *P* value, and a Steel test was used to obtain pair-wise significance by comparing each ABR value to the initial ABR. A *P*-value ≤0.05 was considered statistically significant. All reported *P*-values are two-sided. Analyses were performed using GraphPad Prism version 4 (GraphPad Software, Inc., San Diego, CA, USA), and SPSS version 19.0 software (SPSS Inc., Chicago, IL, USA).

Please cite this article in press as: Naganuma H, et al. Effects of arginine vasopressin on auditory brainstem response and cochlear morphology in rats. Auris Nasus Larynx (2013), http://dx.doi.org/10.1016/j.anl.2013.12.004

Results

In this study, evaluation of hearing impairment in addition to histological assessment after administration of 0.02 unit/g AVP to rats was performed for the first time. The main findings obtained were as follows: (1) hearing impairment occurred, (2) endolymphatic hydrops was not detected histopathologically in the cochlea, (3) vacuoles were observed in the cytoplasm of the intermediate cells of the stria vascularis, and (4) hearing loss of a retrolabyrinthine origin was ruled out.

Hearing impairment

The initial ABR displayed six typical clear peaks in both the control and AVP groups. The averages of the initial ABR thresholds of the control and AVP group were 18 ± 1.3 (SE) dB SPL (range, 10–20 dB SPL) and 16 ± 2.2 dB SPL (range, 10–30 dB SPL), respectively. There was no significant difference ($P = 0.436$, Mann–Whitney U-test).

In the control group, the ABR threshold of each timepoint ranged from 10 to 30 dB SPL with averages of 20 ± 2.6, 22 ± 2.5, 19 ± 2.3, and 20 ± 2.1 dB SPL at 10, 30, 60, and 90 min after injection ($P = 0.406$, Friedman test) (Fig. 1D). The threshold of each ear increased <10 dB SPL in comparison with the initial threshold ($P > 0.05$: Steel test, Fig. 1D-d).

Fig. 1A–C, depict the ABR waves recorded before, 10 min, and 60 min after AVP injection in a representative case. The initial ABR presented six clear peaks (Fig. 1A). The ABR threshold at each timepoint ranged from 10 to 40 dB SPL and the averages were 23 ± 1.5, 23 ± 2.1, 27 ± 2.6, and 25 ± 3.4 dB SPL at 10, 30, 60, and 90 min after injection of AVP (Fig. 1D). ABR thresholds gradually increased up to 60 min and then slightly decreased at 90 min after injection ($P = 0.012$, Friedman test). The ABR threshold significantly increased at 60 min in comparison with the initial threshold ($P < 0.05$, steel test).

The interval time between two latencies of the first and third peak of ABR was not prolonged in rats with impaired hearing. The mean interval times of the initial ABR and ABR at 60 min were 0.952 ± 0.159 (SD) ms and 0.961 ± 0.018 ms, respectively, with no significant difference ($P = 0.654$, Wilcoxon signed-rank test). Therefore, hearing loss of a retrolabyrinthine origin was ruled out.

Histological study of the inner ear

Two representative histological images of the cochlea of the control and AVP groups are shown in Fig. 2. No difference was observed in the morphological aspects of the cochlear duct between the groups. Table 1 presents the Ir-L and Ir-S values of the 2 groups. There was no significant difference ($P > 0.05$, Table 1). Endolymphatic hydrops was not detected in this experiment.

EM of the stria vascularis

The low-magnified images of the stria vascularis in the control and the AVP groups were shown in Fig. 3A, and B, respectively. The marginal, intermediate, and basal cells in the stria vascularis were morphologically normal in the control group (Fig. 3C and E). In the AVP group, however, the vacuole area, which had no cytoplasmic organelles, was expanded in the intermediate cells (Fig. 3D and F) but not in the marginal and basal cells (Fig. 3C and D).

The mean ratio of the total area of defined "vacuoles" in the intermediate cells to the whole area of the stria vascularis was calculated. The ratio was 0.03 ± 0.014 (SE) in rats administered AVP and 0.011 ± 0.006 in the control group. The former value showed a significant increase compared with the latter ($P < 0.01$,

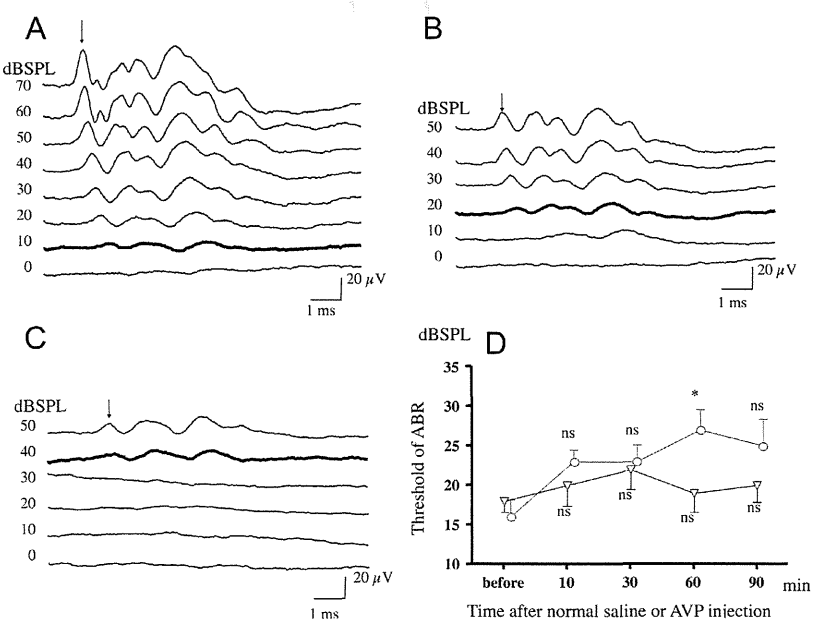

Fig. 1. Hearing assessment after injection of arginine vasopressin (AVP) or isotonic saline solution group. (A–C) A representative auditory brainstem response (ABR) series from the AVP group. The initial ABR showing six clear peaks (A). The ABR threshold, which is indicated as the first peak that disappeared, increased gradually from 10 dB sound pressure level (SPL) to 40 dB SPL at 60 min after AVP ((B and C) recorded at 10 and 60 min after AVP). ABR threshold levels are indicated as a bold wave. (↓) the first peak. (D) ABR thresholds in control and AVP groups. ▽: The average ABR thresholds in the control group show no changes over the series of timepoints ($P = 0.406$: Friedman test, mean ± SE, ns: not significant, Steel test). □: The average ABR thresholds in the AVP group show significantly changes over the series of timepoints ($P = 0.012$: Friedman test, mean ± SE). The average ABR thresholds at 60 min after AVP injection significantly increased in comparison with the initial hearing level (*: $P < 0.05$, ns: not significant: Steel test). Threshold show a gradual increase until 60 min after AVP administration.

Please cite this article in press as: Naganuma H, et al. Effects of arginine vasopressin on auditory brainstem response and cochlear morphology in rats. Auris Nasus Larynx (2013), http://dx.doi.org/10.1016/j.anl.2013.12.004

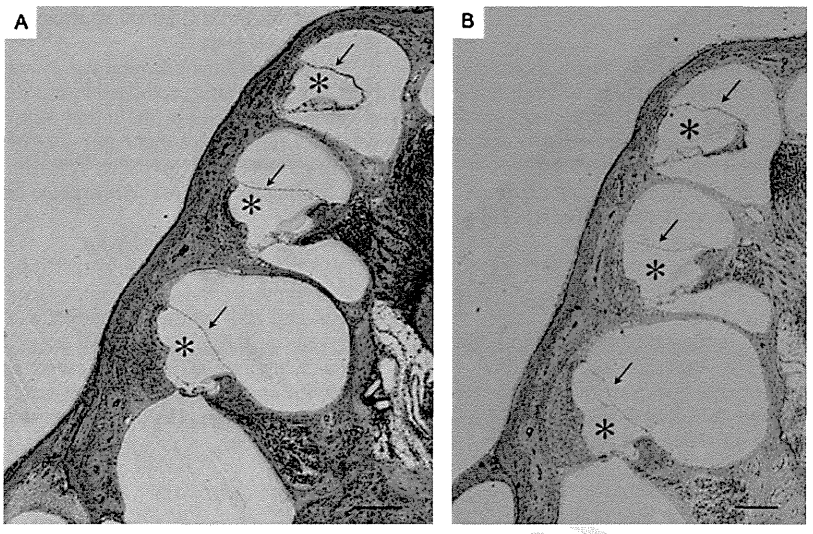

Fig. 2. Histological study of the cochlea to evaluate development of endolymphatic hydrops. Representative pictures of the cochlea in rats from control and AVP groups show the basal, second, and apex turn in the mid-modiolar plane of the cochlea (Control group: (A) AVP group: (B)). Endolymphatic hydrops is not observed in the cochlea after AVP administration. Arrow and asterisk show the Reissner membrane and the endocochlear space (cochlear duct), respectively. Hematoxylin and eosin stain. The bar represents 200 μm.

Mann–Whitney *U*-test, Fig. 3 G). The mean times from euthanasia to fixation of the tissues in the control and AVP groups were 19.2 and 19.6 min, respectively, and were not statistically different ($P > 0.05$, Mann–Whitney *U*-test).

Discussion

The pathology of the inner ear in Meniere's disease can be characterized by endolymphatic hydrops [1,2]. Studies regarding AVP-induced endolymphatic hydrops have been reported [5,7]. Onset and/or reoccurrence of episodic attacks may be provoked by mental or physical stress [11,12], and stress can accelerate secretion of intrinsic AVP [10]. Thus, a putative relationship among mental and/or physical stress, increased AVP secretion, development of endolymphatic hydrops, and occurrence of symptomatic manifestations, such as hearing loss, aural fullness, tinnitus, and vertigo in Meniere's disease exists.

In our study hearing was impaired after administration of 0.02 units/g of AVP to rats. Our findings indicate that an increase in vacuoles in the intermediate cells might be a possible origin of AVP-induced hearing impairment.

Contrary to previous studies [5,7] endolymphatic hydrops was not induced in this experiment. In Kumagami's study [7], the total amount of AVP administered was 10 times the dose administered in our study and guinea pigs were used instead of rats. Takeda and colleagues administered a dose of AVP half of what we used and they provided it to guinea pigs during a 1-week period [5]. These differences in study design might be responsible for inconsistencies in results between our study and theirs.

Despite the fact that endolymphatic hydrops was not observed in our case, hearing impairment was revealed after AVP administration. Endolymphatic pressure might increase without dislocation of Reissner's membrane. According to Tonndorf [13], an elastic bias of the basilar membrane and/or mass loading of the cochlear duct accounts for low-frequency hearing loss; thus, with a pressure rise in the endolymph, hearing loss may occur. If the endolymphatic pressure increased in a range that did not cause Reissner's membrane to bulge, vibration of the basal lamina might be suppressed and hearing might be impaired.

When histopathological changes are analyzed, it is necessary to consider artifacts. In the AVP group, expansion of the area lacking organelles in the cytoplasm of intermediate cells was observed (Fig. 3C and E). A small area of vacuoles in the cytoplasm of intermediate cells was also observed in controls. However, the ratio of the total area of vacuoles in the cytoplasm of the intermediate cells to the whole area of the stria vascularis was significantly increased in the AVP group in comparison with the control group. Thus, it was assumed that an increase in the ratio as a result of AVP administration might be a significant finding.

Previous studies have detailed morphological changes in the stria vascularis following administration of exogenous substances such as bumetanide [14] and furosemide [15]. Although morphological changes represented by vacuole formation in the intermediate cells was induced, as shown in our previous study [16], the

Table 1
Influence on morphological change in scala media.

		Control group			AVP group			*P*-value
		Median	25% Percentile	75% Percentile	Median	25% Percentile	75% Percentile	
Ir-L	Basal turn	0.034	0.015	0.046	0.016	0.008	0.043	0.481
	Second turn	0.044	0.014	0.069	0.034	0.018	0.045	0.630
	Apex turn	0.033	0.019	0.176	0.038	0.008	0.051	0.603
Ir-S	Basal turn	−0.020	−0.101	0.030	−0.005	−0.066	0.042	0.528
	Second turn	−0.019	−0.077	0.041	0.050	−0.017	0.166	0.105
	Apex turn	0.100	0.023	0.158	0.028	−0.004	0.102	0.217

The Ir-S and Ir-L in the AVP group were not significantly different from those in the control group ($P > 0.01$, Mann–Whitney's *U*-test).

Please cite this article in press as: Naganuma H, et al. Effects of arginine vasopressin on auditory brainstem response and cochlear morphology in rats. Auris Nasus Larynx (2013), http://dx.doi.org/10.1016/j.anl.2013.12.004

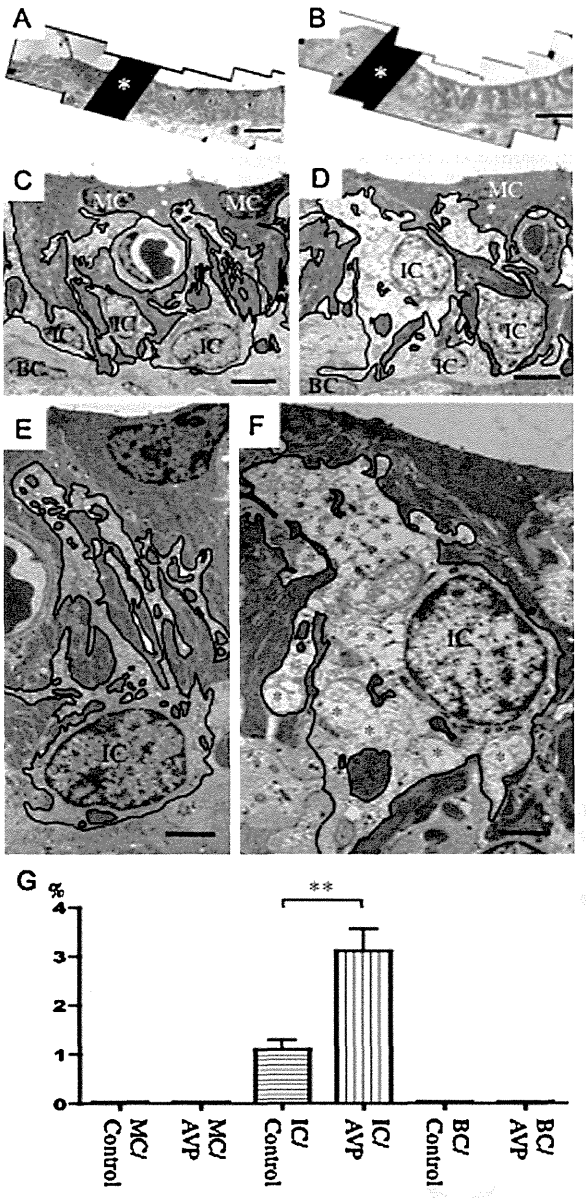

Fig. 3. Representative pictures of the stria vascularis. (A and B): The low-magnified images of the stria vascularis in the control (A) and AVP group (B). The whole stria vascularis was photographed at 2000× magnification using transmission electron microscopy (TEM). The films were scanned at 400 dpi and the images were merged. The black area (asterisk) is a bar of the grid mesh for TEM and the parts of the stria vascularis hidden behind it were excluded from calculation of whole areas of defined "vacuoles" and stria vascularis. The white areas were observed in the stria vascularis in the AVP group. The bar represents 20 μm. (C): Representative pictures of the stria vascularis in the control group: Intermediate, marginal, and basal cells appear histologically normal. Enlargement of the cytoplasm in the intermediate cells is not observed. The cytoplasm in the intermediate cells was thin and organelles were distributed homogeneously. The curved line in the figure indicates the boundary between different cell types. MC: marginal cell, IC: intermediate cell, BC: basal cell, the bar represents 4 μm. (D) Representative picture of the stria vascularis in the AVP group: In the AVP group, the intermediate cell cytoplasm is enlarged with many defined "vacuoles" seen homogenously. The marginal and basal cells were histologically normal. The curved line in the figure indicates the boundary between different cell types. The bar represents 4 μm. (E) Magnified picture of intermediate cells in the control group: The "intermediate cell" was histologically normal. The curved line in the figure indicates the boundary of the intermediate cell. The bar represents 2 μm. (F) Magnified picture of intermediate cells in the AVP group: Many defined "vacuoles" (red asterisks) are observed homogenously in the cytoplasm of the intermediate cells. The curved line in the figure indicates the boundary of the intermediate cell. The bar represents 2 μm. (G) Quantitative analysis regarding vacuoles in each cell: Ratios of the total area of defined "vacuoles" in the cytoplasm of each cell to the whole area of the stria vascularis were compared in the control and AVP groups. In the marginal and basal cells, defined "vacuoles" are not present. In the intermediate cells, the ratio in the AVP group significantly increased in comparison with the control group (**: $P < 0.01$, Mann–Whitney U-test, mean ± SE). MC/Control: marginal cell in the control group, MC/AVP: marginal cell in the AVP group, IC/Control: intermediate cell in the control group, IC/AVP: intermediate cell in the AVP group, BC/Control: basal cell in the control group, BC/AVP: basal cell in the AVP group.

present study's crucial finding may be that excessive AVP administration induced not only morphological changes but also hearing impairment.

The present study agrees with the previous manuscript described by Nishimura et al. [17], but is more precisely evaluated. In our study, the defined vacuoles were increased significantly in the intermediate cells in 60 min after AVP administering. As the ABR thresholds were significantly increased in 60 min after AVP injection, the morphological change in the stria vascularis was investigated at this time point. In their manuscript [17], it was reported that the intrastrial space enlargement in stria vascularis was induced by AVP and it was observed in 20 min after AVP injection then disappeared in 60 min after it. The reason regarding the differences of timepoint and morphological changes was unclear. The possible reasons were, however, thought as follows: (1) The kind of Vasopressin and (2) the route administering AVP were different. In present study, 0.02 unit/g of AVP (Pitressin; Arg-vasopressin, Daiichi-Sankyo, Japan) was administered intraperitoneally. In their one, 50 mg/kg of VP ([Arg8]-vasopressin acetate salt, synthetic; Sigma-Aldrich, Inc., St Louis, MO, USA) was administered subcutaneously. These differences might be related to the speed to absorb AVP and morphological changes.

It has been reported that intermediate cells might play an important role in maintaining endocochlear potential (EP) [18–20]. Vacuoles might cause disorder of oxygen diffusion in intermediate cells [21] and lead to functional disturbances of the Na–K ATPase pump in intermediate cells and Na–K–2Cl cotransporter in marginal cells. Therefore, it is appropriate to consider that vacuole formation in the intermediate cells could degrade the function of intermediate cells and ultimately lead to a decrease in EP.

Mori et al. [22] reported that perilymphatic perfusion of AVP produced an increase in electrical resistance of the scala media concomitant with a drop in EP, suggesting that the main action site of AVP in the cochlea might be the stria vascularis. An increase in electrical resistance in the scala media and a concomitant decrease in EP after administering vasopressin could be the origin of hearing impairment. As a suspected mechanism of hearing impairment in this study, vacuole formation in the intermediate cells might be a substitute pathway of endolymphatic hydrops.

Conclusion

Although the amount of AVP used in this study did not cause endolymphatic hydrops, a significant increase of vacuoles in the intermediate cells of the stria vascularis was revealed. These findings indicate that an increase of vacuoles in the intermediate cells might be a possible origin of AVP-induced hearing impairment. Further studies are needed to investigate the physiological alterations relevant to the morphological changes in the stria vascularis revealed in this study and to examine the effects of AVP receptor antagonists.

Please cite this article in press as: Naganuma H, et al. Effects of arginine vasopressin on auditory brainstem response and cochlear morphology in rats. Auris Nasus Larynx (2013), http://dx.doi.org/10.1016/j.anl.2013.12.004

Acknowledgments

This work was supported in part by Grants-in-Aid for research (C) no. 13671797, no. 15591829, and no. 18591885 from the Ministry of Education, Culture, Sports, Science, and Technology (MEXT) in Japan, Health and Labor Sciences Research Grants of the Ministry of Health, Labor and Welfare Government of Japan regarding research on rare and intractable diseases (vestibular function disorder) in 2007, and a grant from the Graduate School of Medical Science, Kitasato University.

We acknowledge the methodological assistance provided by Dr. T. Katakura (Department of Physiology, Kitasato University School of Medicine), and technical assistance provided by Ms. N. Nemoto (Research Center for Biological Imaging), Mr. S. Yoneda (Department of Otorhinolaryngology, Kitasato University School of Medicine), and Ms. Y. Nakabayashi (Department of Physiology, Kitasato University School of Medicine).

References

[1] Yamakawa K. Uber pathologische Veraenderung bei einem Meniere-kranken. Jpn J Otol 1938;44:2310–2.
[2] Halpike C, Cairns H. Observation on the pathology of Meniere's syndrome. J Laryngol Otol 1938;53:625–55.
[3] Takeda T, Kakigi A, Saito H. Antidiuretic hormone (ADH) and endolymphatic hydrops. Acta Otolaryngol (Stockh) Suppl 1995;519:219–22.
[4] Naganuma H, Kawahara K, Tokumasu K, Okamoto M. Water may cure patients with Meniere disease. Laryngoscope 2006;116:1455–60.
[5] Takeda T, Takeda S, Kitano H, Okada T, Kakigi A. Endolymphatic hydrops induced by chronic administration vasopressin. Hear Res 2000;140:1–6.
[6] Takeda T, Sawada S, Takeda S, Kitano H, Suzuki M, Kakigi A, et al. The effects of V2 antagonist (OPC-31260) on endolymphatic hydrops. Hear Res 2003;182: 9–18.
[7] Kumagami H, Loewenheim H, Beitz E, Wild K, Schwartz H, Yamashita K, et al. The effect of anti-diuretic hormone on the endolymphatic sac of the inner ear. Pflügers Arch 1998;436:970–5.
[8] Kitano H, Suzuki M, Kitanishi T, Yazawa Y, Kitajima K, Isono T, et al. Regulation of inner ear fluid in the rat by vasopressin. Neuro Rep 1999;10:1205–7.
[9] Mhatre AN, Jero J, Chiappini I, Bolasco G, Barbara M, Lalwani AK. Aquaporin-2 expression in the mammalian cochlea and investigation of its role in Meniere's disease. Hear Res 2002;170:59–69.
[10] Lightman SL. The neuroendocrinology of stress: a never ending story. J Neuroendocrinol 2008;20:880–4.
[11] Onuki J, Takahashi M, Odagiri K, Wada R, Sato R. Comparative study of the daily lifestyle of patients with Meniere's disease and controls. Ann Otol Rhinol Laryngol 2005;114:927–33.
[12] Soderman ACH, Moller J, Sjoback DB, Bergenius J, Hallqvist J. Stress as a trigger of attacks in Meniere's disease: a case-crossover study. Laryngoscope 2004;114:1843–8.
[13] Tonndorf J. Endolymphatic hydrops: mechanical causes of hearing loss. Arch Otorhinolaryngol 1976;212:293–9.
[14] Higashiyama K, Takeuchi S, Azuma H, Sawada S, Yamakawa K, Kakigi A, et al. Bumetanide-induced enlargement of the intercellular space in the stria vascularis critically depends on Na+ transport. Hear Res 2003; 186:1–9.
[15] Rybak LP, Whitworth C, Weberg A, Scott V. Effects of organic acids on the edema of the stria vascularis induced by furosemide. Hear Res 1992; 59:75–84.
[16] Naganuma H, Kawahara K, Tokumasu K, Sato R, Ochiai A, Okamoto M. Morphological changes in stria vascularis in animal model after Arg-Vasopressin injection. In: Takeda T, editor. The 2007 annual report of the Research Committee of the Ministry of Health, Labour and Welfare Government of Japan regarding research on intractable diseases (vestibular function disorder). 2008. p. 71–3 (in Japanese).
[17] Nishimura M, Kakigi A, Takeda T, Okada T, Doi K. Time course changes of vasopressin-induced enlargement of the rat intrastrial space and the effects of a vasopressin type 2 antagonist. Acta Oto-Laryngol 2009;129:709–15.
[18] Nin F, Hibino H, Doi K, Suzuki T, Hisa Y, Kurachi Y. The endocochlear potential depends on two K^+ diffusion potentials and an electrical barrier in the stria vascularis of the inner ear. PNAS 2008;105:1751–6.
[19] Hibino H, Nin F, Tsuzuki C, Kurachi Y. How is the highly positive endocochlear potential formed? The specific architecture of the stria vascularis and the roles of the ion-transport apparatus. Eur J Physiol 2010;459:521–33.
[20] Takeuchi S, Ando M, Kakigi A. Mechanism generating endocochlear potential: role played by intermediate cells in stria vascularis. Biophys J 2000;79: 2572–82.
[21] Yamamoto H, Makimoto K. Sensitivity of the endocochlear potential level to cochlear blood flow during hypoventilation. Ann Otol Rhinol Laryngol 2000; 109:945–51.
[22] Mori N, Ohya A, Shugyo A, Matsunaga T. The change in the electrical resistance of the scala media produced by vasopressin. Acta Otolaryngol (Stockh) 1987;104:66–70.

Please cite this article in press as: Naganuma H, et al. Effects of arginine vasopressin on auditory brainstem response and cochlear morphology in rats. Auris Nasus Larynx (2013), http://dx.doi.org/10.1016/j.anl.2013.12.004

Acta Oto-Laryngologica, 2011; 131: 937–944

informa
healthcare

ORIGINAL ARTICLE

Cochlin-tomoprotein (CTP) detection test identifies traumatic perilymphatic fistula due to penetrating middle ear injury

TETSUO IKEZONO[1], SUSUMU SHINDO[1], KUWON SEKINE[1], KYOKO SHIIBA[1], HAN MATSUDA[1], KAORU KUSAMA[1], YASUO KOIZUMI[1], KAZUKI SUGIZAKI[1], SATOMI SEKIGUCHI[2], RYOHEI KATAOKA[1], RUBY PAWANKAR[1], SHUNKICHI BABA[1], TOSHIAKI YAGI[3] & KIMIHIRO OKUBO[1]

[1]*Department of Otorhinolaryngology, Nippon Medical School, Tokyo,* [2]*R&D and Business Development Segment, Mitsubishi Chemical Medience Corporation, Tokyo and* [3]*Chiba Kashiwa Rehabilitation College, Chiba, Japan*

Abstract

Conclusions: The cochlin-tomoprotein (CTP) detection test can be used to make a definite, objective diagnosis of traumatic perilymphatic fistula (PLF), and therefore offers valuable information on patient selection for surgical treatment. *Objectives:* Penetrating middle ear injury can cause traumatic PLF, which is a surgically treatable otologic emergency. Recently, we have reported on CTP, a novel perilymph-specific protein. The purpose of this study was to determine if the CTP detection test is useful for the diagnosis of traumatic PLF. *Methods:* This was a prospective study of CTP detection in penetrating middle ear injury cases with tympanic membrane perforation and hearing loss. *Results:* A total of seven individuals were included in this study. CTP was detected in three of four cases with posterosuperior quadrant perforation of the tympanic membrane. In one of these three cases, even though the high resolution CT scan was not suggestive of PLF and the perilymph leakage could not be visualized intraoperatively, the CTP detection test was able to detect PLF. In two cases, the preoperative positive test results enabled us to make a diagnosis of PLF and a decision for surgical treatment. CTP was not detected in the cases with anterior or inferior tympanic membrane perforation.

Keywords: *Middle ear trauma, hearing loss, COCH gene, cochlin isoform*

Introduction

Penetrating trauma of the middle ear can occur as a result of the introduction of a variety of foreign bodies, for example, a knitting needle, hairpin, bullet, twig of a tree, ear pick, cotton-tipped applicators, stone, and iatrogenic damage [1–9]. Trauma associated with the ossicular chain is a frequent finding in these cases and carries a good prognosis. Inner ear damage, however, while less frequent, exposes the patient to permanent disabilities in hearing and vestibular function.

Etiologies of inner ear damage due to penetrating middle ear injury include labyrinthine concussion, acoustic trauma, and perilymphatic fistula (PLF) [10–12]. Among these conditions, PLF is an otologic emergency and is surgically correctable by sealing the fistula. Appropriate recognition and treatment of PLF can improve hearing and balance in the afflicted patients; otherwise, permanent deafness may result [2]. In the absence of high resolution CT scan (HRCT) findings suggestive of PLF, such as otic capsule fracture, stapes luxation or pneumolabyrinth, it is difficult to make a definite, objective diagnosis of PLF.

Recently, we reported our findings on cochlin-tomoprotein (CTP), a novel perilymph-specific protein. By proteomic analysis of inner ear proteins, certain unique properties of cochlin isoforms were discovered. We detected three cochlin isoforms, p63s, p44s, and p40s, in the inner ear tissue and a short

Correspondence: Tetsuo Ikezono MD PhD, Department of Otorhinolaryngology, Nippon Medical School, 1-1-5, Sendagi, Bunkyo-ku, Tokyo 113-8603, Japan. Tel: +81 3 3822 2131, Tel: ext. 6746. Fax: +81 3 5685 0830. E-mail: ctp16kdaplf@nms.ac.jp

(Received 2 February 2011; accepted 20 March 2011)

ISSN 0001-6489 print/ISSN 1651-2251 online
DOI: 10.3109/00016489.2011.575795

16 kDa isoform, named cochlin-tomoprotein (CTP), in the perilymph [13,14]. CTP was selectively expressed only in the perilymph, not in cerebrospinal fluid (CSF), saliva or serum on testing 65, 60, 29, and 28 samples, respectively [14–16].

We have reported a standardized CTP detection test for the diagnosis of PLF, using a spiked standard of recombinant human (rh)CTP on Western blot [17].

Using this diagnostic method, we detected CTP in three of seven cases of penetrating middle ear injury. To the best of our knowledge this is the first definite diagnosis of traumatic PLF using CTP as the diagnostic marker.

Material and methods

Study design and participants

The participants in this investigation were derived from the patients who had been consecutively referred to the first author's outpatient clinic. Enrolment took place from June 2003 to December 2007, and patients were included based on a history of insertion of an object into the middle ear, tympanic membrane perforation, and accompanying hearing loss with or without balance disorders. A total of seven patients were enrolled in this study. An ear pick caused injury while removing cerumen (a common practice in Japan) in cases 1–5 and 7. A screwdriver was accidentally inserted into the ear of case 6.

We performed physiological testing by pure tone audiometry and nystagmoscopy with infrared radiation. HRCT was performed in all cases. In this study, HRCT findings suggestive of PLF are defined as otic capsule fracture, pneumolabyrinth (vestibulum or cochlea), ossicular dislocation of the stapes or incudostapedial joint. Fistula test (applying positive and negative pressure to the middle ear) was not performed to avoid further damage of the inner ear.

Standardized CTP detection test by Western blot

Samples were tested by the standardized CTP detection test [17] with minor modifications. For Western blot analysis, the rabbit polyclonal anti-CTP antibody (formerly anti-LCCL-C Ab) was prepared as described previously. In brief, a 14-mer peptide (LSRWSASFTVTKGK) corresponding to residues 114–127 in the LCCL domain was used as an antigenic peptide to generate antibody. The rhCTP was used as a spiked standard on Western blot. A putative CTP sequence predicted from our previous study, the 101 to 403 positions of the cDNA corresponding to amino acid residues 32–132, was amplified by PCR from a human expressed sequence tag clone, IMAGE ID 27789 (Kurabo, Japan). rhCTP was produced using pCR/T7/TOPO/TA Expression Kits (Invitrogen).

Samples were loaded onto 15% polyacrylamide gels and transferred onto PVDF membranes. Membranes were blocked overnight at 4°C in 5% skim milk and 0.2% polyoxyethylenesorbitan (Tween-20) dissolved in phosphate-bufferd saline (PBS; pH 7.5). Membranes were then incubated in PBS containing 1% skim milk and 0.1% Tween-20 for 2 h at room temperature with the primary antibody (anti-CTP antibody) diluted at 1:2000. After washing with 0.05% Tween-20 in PBS, membranes were incubated for 1 h at room temperature with horseradish peroxidase-labeled goat anti-rabbit IgG antibody (Dako, Japan) diluted at 1:10 000 in the same buffer as used for the primary antibody reaction. They were washed again and the reaction was developed with a chemiluminescence reaction kit (ECL Advance, Amersham), and then analyzed by an image analyzer LAS-3000 (Fuji Film, Japan). Tests were performed and analyzed by well-trained personnel who did not have any information on the clinical background of the patients.

The detection limit of the serially diluted rhCTP was between 0.27 and 0.13 ng/well. These two amounts of rhCTP were set as the high and low spiked standards, respectively, and were the amounts electrophoresed each time when we tested the samples. When the intensity of the band in the samples tested was below the high standard signal, the result was considered to be negative. The low spiked standard was used to estimate the protein transfer efficiency.

Test results were expressed qualitatively (positive or negative) by the presence or absence of the anti-CTP antibody reacting protein with the molecular weight, which exactly matched the molecular weight of native CTP (16 kDa) on Western blot. The result of the CTP detection test was provided to the clinic within 4 days of sampling.

Performance of the CTP detection test

The performance of the CTP detection test was described previously [17]. In brief, the detection limit of perilymph was 0.161 μl per lane in an average of five samples. This means that the test can detect CTP if there is 3.3 μl of perilymph in 0.3 ml of middle ear lavage (MEL) (explained in detail by Ikezono et al. [17]). We also studied the stability of CTP protein when samples were stored at room temperature (25°C) or 4°C for as long as 55 days. The effect of repeated freezing and thawing was also evaluated. The

results showed that CTP is a stable protein and detection is not affected by the storage condition or repeated freezing and thawing [16].

We also reported the specificity of the CTP detection test by testing non-PLF cases [17]. We defined 'non-PLF' as those cases with otosclerosis (that had undergone stapedectomy), profound deafness (cochlear implant surgery), or conductive hearing loss (exploratory tympanotomy) without any sign of inflammation or infection. We took MEL before the stapedectomy or cochleostomy, or before surgical treatment of conductive hearing loss. The MEL in 54 of 55 non-PLF cases was negative with the CTP detection test, i.e. the specificity of the test was found to be 98.2%. To further elucidate the limitations to this test, we analyzed the MEL collected from patients with middle ear infections, which can give a false-positive result. The MEL in 43 of 46 cases with chronic suppurative otitis media or middle ear cholesteatoma was negative for CTP. The specificity of the CTP detection test decreases to 93.5% when applied to inflamed and infected ears. The high protein concentration of the thick pus present with infection was the most likely cause. In the present investigation inflamed ears were studied, so the specificity is thought to be due to the latter. These findings indicate that CTP can be considered a marker for the diagnosis of PLF.

Sampling method

We aimed to establish an easy-to-perform sampling method. Samples were collected by lavaging the middle ear cavity four times with the same bolus of 0.3 ml of saline and recovering the fluid. This was defined as middle ear lavage (MEL). In the outpatient clinic, MEL was collected through a perforated tympanic membrane (cases 3–7), or at myringotomy in case 2 whose traumatic tympanic membrane perforation had been closed during the 27 day period between the onset and the first visit to our clinic. MEL was also collected during surgery in cases 1–3. Hence, in cases 2 and 3, MEL was collected twice (before and during operation) and we could test whether the leakage continued during these two sampling time points. Samples were centrifuged at 1250 *g* for 1 min and the supernatants were frozen and stored at –80°C until use. Sixteen µl of MEL were mixed with 8 µl of three times concentrated sample buffer (150 mM Tris-HCl (pH 6.8), 6% SDS, 30% glycerol, 0.3% bromophenol blue, 300 mM DTT) for Western blot analysis. All patients gave their full informed consent and the study was approved by the Ethics Committee of Nippon Medical School.

Therapeutic procedure

All cases except for cases 4 and 5 received tapering doses of oral prednisolone (60–30 mg) down to 5 mg in an 8–14 day period depending on the patient's general condition and any other systemic illnesses. Surgery (exploratory tympanotomy and PLF repair surgery) was performed under general anesthesia in cases 1–3, in order to inspect and seal the potential perilymph leak from the fistula and to reconstruct the ossicular chain (explained in detail in the Results section). Conservative treatment (medication and bedrest) was selected in cases 4–7 and tympanic membrane perforation was closed with patching.

Evaluation of the therapeutic outcome

Pure tone audiogram was obtained before and after treatment. The pure tone average (PTA) hearing thresholds of bone conduction and air conduction were determined by four frequencies (500, 1000, 2000, and 4000 Hz). The patients were followed up regularly and PTA was performed until complete recovery, or for more than 2 months (average 8 months). Hearing improvement after treatment was gauged by PTA of air conduction using the following criteria; CR, complete recovery (final audiogram ≤20 dB HL, or improvement to the same degree of hearing as the unaffected ear); RI, remarkable improvement (improvement >30 dB HL); I, improvement (improvement of 10–30 dB HL); NC, no change or deterioration (improvement <10 dB HL) (modified from Kanzaki et al. [18]). Successful hearing improvement was defined as complete recovery or remarkable improvement.

Results

The patient information and test results (age, sex, affected side, HRCT suggestive of PLF, CTP test results, onset to MEL sampling (days), site of perforation, pre- and post-treatment PTA, air–bone gap, hearing improvement, nystagmus) are summarized in Table I. Representative Western blot analysis of CTP detection in MEL from cases 2, 3, and 7 are shown in Figures 1 and 2. None of these cases presented with infection in the middle ear. The contralateral ear exhibited normal hearing in all cases. Successful hearing improvement (complete recovery or remarkable improvement) was achieved in all cases except in case 7. Vertigo, as a sign of inner ear damage, was observed in cases 1–4, and disappeared in all cases during the follow-up period. In cases 5–7, perforation was not in the posterosuperior quadrant (PSQ) and CTP was negative (Figure 2), suggesting

Table I. Summary of patient information and test results.

	Case no.						
Parameter	1	2	3	4	5	6	7
Age	54	29	7	27	28	39	48
Sex	F	F	M	F	F	M	M
Affected side	L	L	R	L	R	L	L
HRCT suggestive of PLF	+	+	–	–	–	–	–
CTP test results	+	+, +	+, +	–	–	–	–
Onset to MEL sampling (days)	8	27, 35	2, 9	1	4	1	1
Site of perforation	PSQ	PSQ	PSQ	PSQ	Inferior	Anterior	Anterior
Pretreatment bone PTA	33	20	5	35	14	20	35
Pretreatment air PTA	65	70	20	56	40	58	56
Pretreatment ABG	32	50	15	21	26	38	21
Post-treatment Bone PTA	20	19	3	24	11	15	28
Post-treatment air PTA	23	33	10	36	15	19	36
Post-treatment ABG	3	14	8	13	4	4	9
Hearing improvement	RI	RI	CR	CR	CR	CR	I
Nystagmus	S	S, P	S	S, P, BPPV	–	P	S

Middle ear lavage (MEL) was collected only once except in cases 2 and 3, where MEL was taken twice preoperatively and during the operation. +, +, CTP detection test was performed twice and both results were positive. ABG, air–bone gap; BPPV, benign paroxysmal positional vertigo; CR, complete recovery; CTP, cochlin-tomoprotein; HRCT, high resolution CT scan; I, improvement; MEL, middle ear lavage; NC, no change or deterioration; P, rotatory and horizontal, paretic; PLF, perilymphatic fistula; PSQ, posterosuperior quadrant; PTA, pure tone average; RI, remarkable improvement; S, rotatory and horizontal, stimulatory.

that the inner ear damage could be attributed to non-PLF causes. Therefore, in the following section we focus on discussing cases 1–4.

Case 1 had mixed hearing loss and developed severe rotatory vertigo 36 h after the traumatic event. HRCT exhibited pneumolabyrinth in the vestibulum and dislocation of the incudostapedial joint. The stapedial footplate seemed to be in an intact position. The intraoperative findings showed that the stapes annular ligament was lax with excess mobility of the stapes. The stapedial footplate was slightly elevated (probably an ear pick with a spoon-like tip lifted the stapes when the patient pulled it out after penetration, as shown by Kobayashi and Gyo [1]). Perilymph leakage was detected, the stapes was replaced after coverage of the oval window with fascia, and the ossicular chain was reconstructed. The MEL performed intraoperatively was positive for CTP. The PTA demonstrated remarkable hearing improvement after surgery (Figure 3a).

Case 2 was referred to our clinic because of sustained conductive hearing loss and vertigo for 1 month post injury. HRCT revealed stapes luxation and air in the vestibulum. MEL was taken on the 35th day and CTP was detected (Figure 1), suggesting that the perilymph had been continuously leaking out and/or had pooled in the middle ear cavity for 35 days without remarkable exacerbation of the sensorineural component of hearing loss. During surgery, perilymph leakage was detected and the stapes was smoothly taken out through the oval window. The ossicular chain was reconstructed with a Teflon piston and the oval window was covered with fascia to seal the perilymphatic leakage. MEL taken intraoperatively was positive for CTP. The PTA demonstrated remarkable hearing improvement post surgery (Figure 3b).

Case 3 had severe rotatory vertigo 10 h after the traumatic event and mild conductive hearing loss (Figure 3c). HRCT did not exhibit any findings suggestive of PLF. MEL taken on the second day after the event showed positive CTP expression (Figure 1). Due to the traumatic PLF and the possibility that the hearing might worsen, surgery was performed on the ninth day. Intraoperatively, the stapes annular ligament was lax with excess mobility of the stapes, and there was slight dislocation of the incudostapedial joint. Granulation was observed around the stapes without identifiable leakage of perilymph. MEL taken intraoperatively was positive for CTP. The oval window was sealed with fascia and fibrin glue and the incudostapedial joint was reconstructed. The audiometric findings were normal and there was no vertigo post surgery (Figure 3c). The

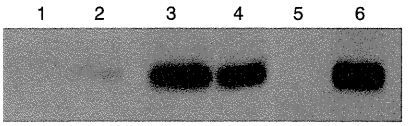

Figure 1. The middle ear lavage (MEL) samples collected preoperatively from cases 2 and 3 were tested by Western blot using anti-cochlin-tomoprotein (CTP) antibody to detect CTP. The MEL from both cases 2 and 3 shows a positive result. Lane 1, rhCTP low spiked standard (0.13 ng/well), CTP-negative; 2, rhCTP high spiked standard (0.27 ng/well), CTP-positive; 3, 16 µl of MEL from case 3, CTP-positive; 4, 2 µl of perilymph (positive control), CTP-positive; 5, blank, CTP-negative; 6, 16 µl of MEL from case 2, CTP-positive.

MEL samples taken preoperatively and at surgery were both positive for CTP, indicating that the perilymph was still leaking out and/or had pooled in the middle ear cavity for 8 days.

In case 4, perforation was in the PSQ, but the HRCT finding was not suggestive of PLF and the CTP was negative. The vertigo and hearing loss resolved with conservative treatment.

Discussion

Penetrating middle ear injuries are reportedly commonly caused by the insertion of various kinds of foreign objects. These foreign objects result in perforation of the tympanic membrane, ossicular dislocation or, most seriously, direct damage to the stapes. In Japan, removing the cerumen by an ear pick is a common practice, and there were 20 cases of penetrating middle ear injuries reported over a 10-year period [1]. The current report comprises the largest number of middle ear injury cases (seven cases) in a single study.

We would like to emphasize that even though it is not a common trauma, penetrating middle ear injury is a very important condition for understanding the pathomechanisms of traumatic inner ear injuries. An improved understanding will enable therapeutic and preventative strategies for acute, late onset, and debilitating neuro-otological problems of patients with similar pathomechanics, such as temporal bone fracture, pneumolabyrinth or iatrogenic injuries during otologic surgery.

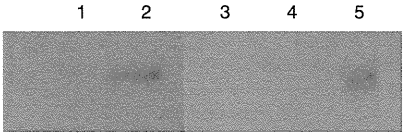

Figure 2. The middle ear lavage (MEL) sample from case 7 was tested by Western blot using anti-cochlin-tomoprotein (CTP) antibody to detect CTP, which shows a negative result. Lane 1, rhCTP low spiked standard (0.13 ng/well), CTP-negative; 2, rhCTP high spiked standard (0.27 ng/well), CTP-positive; 3, blank, CTP-negative; 4, 16 µl of MEL from case 7, penetrating middle ear injury, CTP-negative; 5, 0.25 µl of perilymph (positive control), CTP-positive.

Symptoms commonly associated with this type of injury include acute hearing loss, vertigo, tinnitus, and pressure sensation in the affected ear. The severity of the injury was first analyzed by the symptoms and test results such as HRCT findings, audiogram, and nystagmus. Inner ear damage can have various etiologies, such as labyrinthine concussion, acoustic trauma or PLF [10–12]. Conservative treatment is adequate for labyrinthine concussion and acoustic trauma, but traumatic PLF is an otologic emergency that may require surgical treatment. Appropriate recognition and treatment of PLF is especially important and it can improve hearing and balance, and hence the quality of life of the afflicted patients.

However, differential diagnosis among these various etiologies is not a simple task. This has led to a series of research efforts to identify an endogenous marker of perilymph [14]. Previously beta2-transferrin was thought to be a marker; however, a more recent study showed that, because of the relative amount of serum and perilymph in a mixed sample, electrophoretic separation of the transferrin variant might not be diagnostic [19]. As explained in the Methods section, we have shown that CTP was selectively detected in the perilymph and established a standardized CTP detection test for the diagnosis of PLF, using a spiked standard of rhCTP on Western blot [15–17]. We have reported the performance of the CTP detection test, including the specificity of the test and the stability of the CTP protein.

In the present study, we have shown the usefulness of the CTP detection test for the diagnosis of traumatic PLF in the clinical setting. In four middle ear trauma cases suspected to have stapes injury due to the symptoms and the site of perforation (i.e. the PSQ), three cases had a positive CTP detection test (cases 1–3). When the site of perforation was in the PSQ and HRCT detected pneumolabyrinth, a diagnosis of traumatic PLF due to the direct injury to the stapes was made, as in cases 1 and 2. Even HRCT was not clearly indicative of PLF, since it was the CTP detection test that enabled the detection of PLF in case 3. If the site of perforation and HRCT findings are not suggestive of PLF, a negative CTP result can thus help to exclude PLF, as in cases 5–7.

The conventional gold standard for PLF detection is the intraoperative microscopic visualization of perilymph leakage and fistula [17]. By this intraoperative microscopic visualization, a definitive diagnosis of

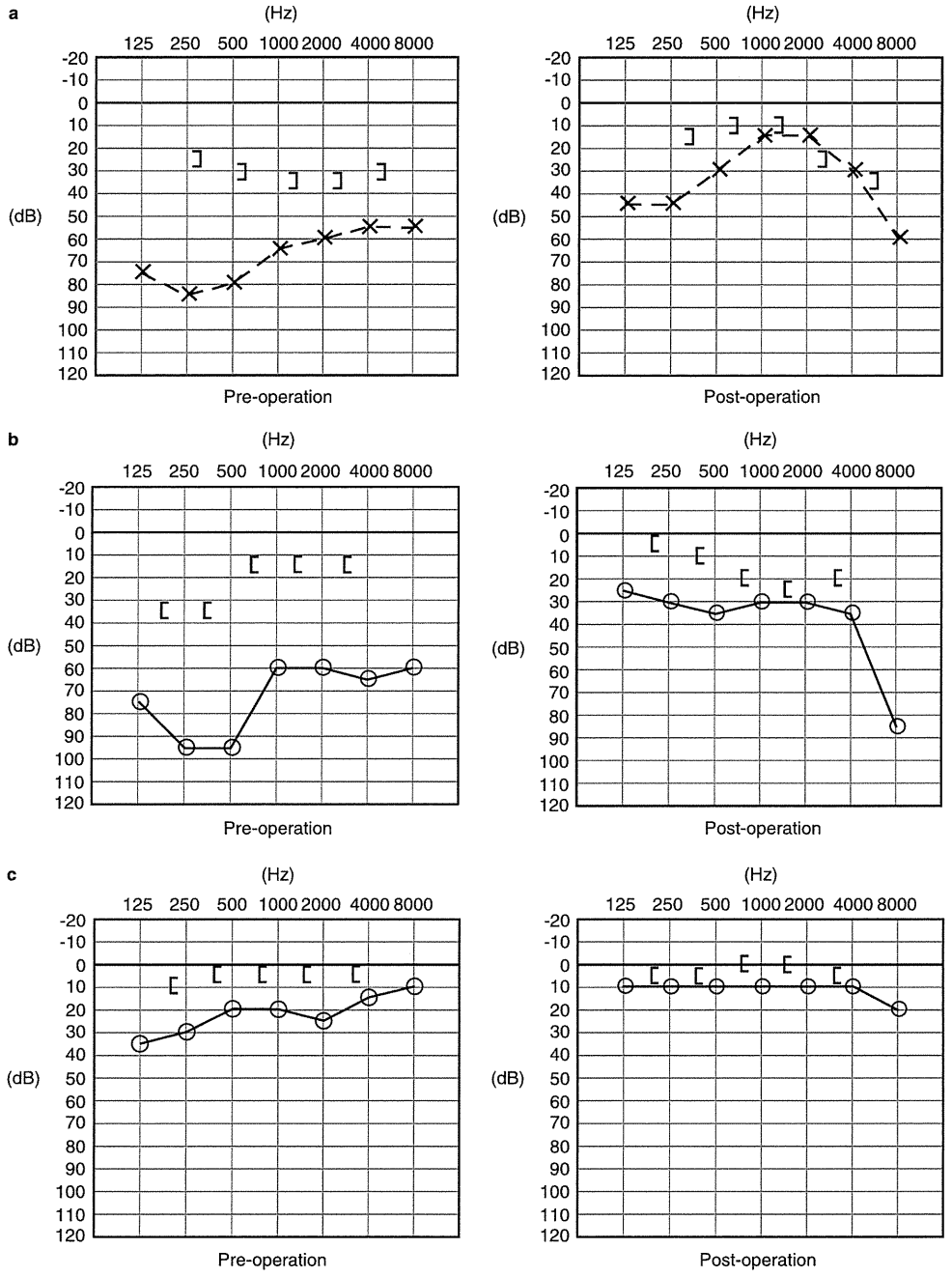

Figure 3. Pre- and post-treatment pure tone audiograms of case 1 (a), case 2 (b), and case 3 (c), with positive CTP detection test results.

traumatic PLF was made in both cases 1 and 2, and the CTP positive result confirmed this. In case 3, the oval window fistula and leakage were not apparent, even though the annular ligament was identified as lax with excess mobility. Even in this type of ambiguous condition, the CTP detection test was able to clearly identify PLF. In these cases with a positive CTP test result, severe rotatory vertigo was one of the main complaints. Even if the hearing loss was stable or had not deteriorated remarkably, the presence of

vestibular symptoms is important for an accurate diagnosis.

The preoperative CTP detection test was valuable for the decision as to the need for surgery in cases 2 and 3. In chronic cases such as case 2, the key question is whether the perilymph leakage persists or not due to spontaneous healing with granulation formation in the oval window. When the leakage ceases, conservative treatment is indicated. When the leakage persists, surgical treatment (sealing the fistula and reconstruction of ossicular chain) is needed to prevent inner ear infection, meningitis or further deterioration of the inner ear dysfunction. On the other hand, with mild traumatic PLF as in case 3, sealing the damaged annular ligament can be performed without serious complications.

We were able to achieve improvement in both hearing and vestibular symptoms in cases 1–3. However, surgical treatment is still a controversial issue in these types of stapes injury. Hearing and vestibular function vary after surgical treatment due to the initial degree of inner ear damage caused by the injury, and the additional effect caused by the surgical procedure itself, which may further damage the inner ear.

Conclusion

The CTP detection test enabled a definite diagnosis of traumatic PLF among penetrating middle ear injury cases. These PLF cases, which were definitely diagnosed with the positive CTP test results, revealed the patient symptoms and physiological test results to be widely variable. The inner ear damage may be dependent upon the rapidity of onset, duration of the perilymph leakage, the site of the leakage, and other biological factors. Using this CTP detection test, a definitive diagnosis of PLF can be made and appropriate therapeutic options for this surgically correctable disease can be taken into consideration. Further studies will be needed to provide insight into the etiology and pathomechanisms, and such insight may lead to the development of therapeutic and preventative strategies for acute, late onset, and debilitating neuro-otological problems.

Acknowledgments

We thank Dr Shin-Ichi Haginomori, Department of Otorhinolaryngology Osaka Medical College, Dr Hideki Matsuda, Department of Otorhinolaryngology, Yokohama City University School of Medicine, and Dr Hiroshi Ogawa, Department of Otorhinolaryngology, Fukushima Medical University, for their generous cooperation. This study was supported by Health and Labor Sciences Research Grants in Japan (Research on Measures for Intractable Diseases, Researches on Sensory and Communicative Disorders), a grant from the Ministry of Education, Culture, Sports, Science and Technology. Nippon Medical School and Mitsubishi Chemical Corporation have Japanese patent on this test. Nippon Medical School has Chinese, Australian, European, and US patent. None of the authors have received any financial compensation for their work.

Declaration of interest: The authors report no conflicts of interest. The authors alone are responsible for the content and writing of the paper.

References

[1] Kobayashi T, Gyo K. Earpick injury of the stapes. Am J Otolaryngol 2000;21:340–3.
[2] Vanderstock L, Vermeersch H, De Vel E. Traumatic luxation of the stapes. J Laryngol Otol 1983;97:533–7.
[3] Herman P, Guichard JP, Van den Abbeele T, Tan CT, Bensimon JL, Marianowski R, et al. Traumatic luxation of the stapes evidenced by high-resolution CT. AJNR Am J Neuroradiol 1996;17:1242–4.
[4] Yamasoba T, Amagai N, Karino S. Traumatic luxation of the stapes into the vestibule. Otolaryngol Head Neck Surg 2003; 129:287–90.
[5] Lao WW, Niparko JK. Assessment of changes in cochlear function with pneumolabyrinth after middle ear trauma. Otol Neurotol 2007;28:1013–17.
[6] Hatano A, Rikitake M, Komori M, Irie T, Moriyama H. Traumatic perilymphatic fistula with the luxation of the stapes into the vestibule. Auris Nasus Larynx 2009;36:474–8.
[7] Snelling JD, Bennett A, Wilson P, Wickstead M. Unusual middle-ear mischief: trans-tympanic trauma from a hair grip resulting in ossicular, facial nerve and oval window disruption. J Laryngol Otol 2006;120:793–5.
[8] Ederies A, Yuen HW, Chen JM, Aviv RI, Symons SP. Traumatic stapes fracture with rotation and subluxation into the vestibule and pneumolabyrinth. Laryngoscope 2009;119:1195–7.
[9] Meriot P, Veillon F, Garcia JF, Nonent M, Jezequel J, Bourjat P, et al. CT appearances of ossicular injuries. Radiographics 1997;17:1445–54.
[10] Schuknecht HF. Mechanism of inner ear injury from blows to the head. Ann Otol Rhinol Laryngol 1969;78: 253–62.
[11] Fitzgerald DC. Head trauma: hearing loss and dizziness. J Trauma 1996;40:488–96.
[12] Ohlemiller KK. Recent findings and emerging questions in cochlear noise injury. Hear Res 2008;245:5–17.
[13] Ikezono T, Omori A, Ichinose S, Pawankar R, Watanabe A, Yagi T. Identification of the protein product of the Coch gene – hereditary deafness gene – as the major component of bovine inner ear protein. Biochim Biophys Acta 2001;3:258–65.
[14] Ikezono T, Shindo S, Li L, Omori A, Ichinose S, Watanabe A, et al. Identification of a novel Cochlin isoform in the perilymph: insights to Cochlin function and the pathogenesis of DFNA9. Biochem Biophys Res Commun 2004; 6:440–6.

[15] Ikezono T, Shindo S, Sekiguchi S, Hanprasertpong C, Li L, Pawankar R, et al. Cochlin-tomoprotein (CTP), a novel perilymph-specific protein and a potential marker for the diagnosis of perilymphatic fistula. Audiol Neurotol 2009; 14:338–44.

[16] Ikezono T, Sugizaki K, Shindo S, Sekiguchi S, Pawankar R, Baba S, et al. Temporal analysis of profuse fluid leakage (gusher) from cochleostomy. Acta Otolaryngol 2010;130: 881–7.

[17] Ikezono T, Shindo S, Sekiguchi S, Morizane T, Pawankar R, Watanabe A, et al. The performance of CTP detection test for the diagnosis of perilymphatic fistula. Audiol Neurootol 2009;15:168–74.

[18] Kanzaki J, Inoue Y, Ogawa K, Fukuda S, Fukushima K, Gyo K, et al. Effect of single-drug treatment on idiopathic sudden sensorineural hearing loss. Auris Nasus Larynx 2003;30:123–7.

[19] Rauch SD. Transferrin microheterogeneity in human perilymph. Laryngoscope 2000;110:545–52.

Acta Oto-Laryngologica, 2012; 132: 1134–1139

informa
healthcare

ORIGINAL ARTICLE

Cochlin expression in the rat perilymph during postnatal development

KYOKO SHIIBA[1], SUSUMU SHINDO[2], TETSUO IKEZONO[2], KUWON SEKINE[1], TOMOHIRO MATSUMURA[3], SATOMI SEKIGUCHI[4], TOSHIAKI YAGI[5] & KIMIHIRO OKUBO[1]

[1]*Department of Otorhinolaryngology, Nippon Medical School, Tokyo,* [2]*Department of Otorhinolaryngology, Saitama Medical University Faculty of Medicine, Iruma, Saitama,* [3]*Department of Biochemistry and Molecular Biology, Nippon Medical School, Tokyo,* [4]*R&D and Business Development Segment, Mitsubishi Chemical Medience Corporation, Tokyo and* [5]*University of Human Environments, Okazaki, Aichi, Japan*

Abstract

Conclusions: The changes in the cochlin isoforms in the perilymph may provide important insights to the understanding of cochlin function and the pathogenesis of related inner ear diseases. *Objectives*: Cochlin is involved in various pathologies of the inner ear. Altered levels of cochlin isoforms in developing inner ear tissue were reported previously. The purpose of this study was to elucidate the cochlin isoform expression in the perilymph of rats during postnatal development in relation to Coch gene mRNA expression. *Methods*: We studied the cochlin isoforms in the rat perilymph during postnatal development by Western blot analysis. Real-time PCR was also performed to elucidate the expression level of Coch mRNA in the developing inner ear of rats. *Results*: Western blot analysis showed that the expression of p63s in the perilymph was highest on the 12th day after birth (DAB12), the earliest age at which we could identify the perilymphatic space microscopically, and it decreased gradually as the cochlea developed. On the other hand, the expression of Cochlin-tomoprotein (CTP)was lowest on DAB12 and increased gradually up to DAB24. COCH mRNA was detected from DAB3 and gradually increased to DAB15, and then gradually decreased to DAB70.

Keywords: *DFNA9, COCH gene, Western blot, real-time PCR*

Introduction

The COCH (coagulation factor C homology) gene, which encodes the abundant inner ear protein cochlin, has been shown to be mutated in the autosomal dominant, late-onset, and progressive nonsyndromic hearing loss and vestibular disorder DFNA9. To date, 13 different missense mutations and one in-frame deletion have been reported in patients [1–4]. Balance problems, vertigo, positional nystagmus, dizziness, tinnitus, night blindness, memory loss, and cardiovascular diseases have been reported in the affected family members [5,6]. Cochlin is also a prominent target antigen in CD4+ T-cell-mediated autoimmune hearing loss [7]. Additionally, increased levels of cochlin have been found in the trabecular meshwork of glaucomatous mice and are presumed to have a causal role in the development of increased intraocular pressure and glaucoma [8]. Cochlin is thus clearly involved in various pathologies of the inner ear and eye. However, the precise mechanisms underlying the pathogenesis and the function of the cochlin protein, the most highly expressed protein in the human and mouse inner ear, at present still remain unclear.

We have conducted a series of studies to elucidate the cochlin isoforms and the mechanism of expression. The three cochlin isoforms p63s, p44s, and p40s, were detected in the inner ear tissue and a short 16 kDa isoform, Cochlin-tomoprotein (CTP), was

Correspondence: Tetsuo Ikezono MD PhD, Department of Otorhinolaryngology, Saitama Medical University Faculty of Medicine, Iruma, Saitama 350-0495, Japan. Tel: +81 49 276 1253. Fax: +81 49 295 8061. E-mail: ikez@saitama-med.ac.jp

(Received 26 February 2012; accepted 14 April 2012)

ISSN 0001-6489 print/ISSN 1651-2251 online © 2012 Informa Healthcare
DOI: 10.3109/00016489.2012.687456

found in the perilymph [9,10]. We also show that dynamic changes occur in cochlin isoform expression during postnatal development in the rat inner ear. Both immunohistochemistry and Western blot analysis showed an increase in the expression of the total amount of cochlins [11] during development. The level of expression of p63s was the highest among the three isoforms between the 17th day after birth (DAB17) and DAB24. In contrast, on DAB70, the expression of p63s had decreased and p40s had become the predominant isoform. The importance of isoform analysis was reported in a study of Usher syndrome type 1F (USH1F) [12], where altered levels of cochlin isoforms were suggested to be pathogenic.

To determine how expressions of COCH isoforms are controlled, we investigated the perilymph in this study. Contrary to expectations, Western blot analysis showed that the expression of p63s in the perilymph was the highest on DAB12, the earliest age at which the perilymphatic space could be visualized microscopically, and decreased gradually as the cochlea developed. On the other hand, the expression of CTP was lowest on DAB12 and increased gradually to DAB24. Coch mRNA was detected on DAB3. This study demonstrates the temporal changes in the expression of the cochlin isoforms in the perilymph of the developing ear of the rat.

Material and methods

Animals

For real-time PCR, the inner ear membranous labyrinth was excised from Wistar rats (Sankyo Labo Service Corporation, Tokyo, Japan) including the temporal bones on DAB3 and DAB6 (n = 20 ears for each group), as well as DAB 9, 12, 15, 24, 36, and 70 (n = 10 ears for each group), and the samples were mixed in each group. The perilymph was collected as follows. Under microscopy, after removing the stapes, the perilymphatic space was identified and the perilymph was suctioned out slowly with a thin pipette, taking special care not to touch or damage the membranous labyrinth. In the preliminary stage of the experiment, we investigated the identification of the perilymphatic space, and DAB12 was the youngest age at which perilymph could be collected. Wistar rats on DAB12 and 18 (n = 8 ears for each group) as well as DAB 24, 30, and 70 (n = 4 ears for each group) were used for Western blot analysis of the perilymph and the samples were mixed for each group.

For the performance of the experimental procedure, each rat was deeply anesthetized with sodium pentobarbital (50 mg/kg, i.p.) This study was approved by the Animal Experimentation Ethics Committee (No. 19-108, approved on May 16, 2008) of Nippon Medical School.

Western blot

Since human, bovine, and rat perilymph contains two cochlin isoforms, the full-length isoform p63 and the short truncated isoform CTP, we used the rabbit polyclonal anti-LCCL-C Ab (Figure 1), which recognizes these isoforms [10,13]. This antibody was prepared as described previously [10]. In brief, a 14-mer peptide (LSRWSASFTVTKGK) corresponding to residues 114–127 of the LCCL (Limulus factor C, Coch-5b2, and Lgl1) domain was used to generate the antibody. We added cysteine residues to the C termini of the peptides to permit coupling of the peptides to KLH as a carrier protein for immunization. Rabbits were immunized by repeated subcutaneous injections of the KLH-coupled peptides. The serum was purified using a protein A column, followed by peptide-affinity chromatography. The specificity of the antibodies for the corresponding antigenic peptides was confirmed by dot-blot analysis and a peptide absorption test (data not shown).

The perilymph was centrifuged at 1000 *g* for 15 min and the supernatant was stored at –80°C until use. Then 0.5 µl of each perilymph sample was loaded onto a 15% SDS-polyacrylamide gel. Before loading, samples were diluted with 0.188 M Tris buffer to a total volume of 10 µl and mixed with 5 µl of sample buffer (0.188 M Tris buffer, 2.39 mM SDS, 30% glycerol, and 15% 2-mercaptoethanol). The samples

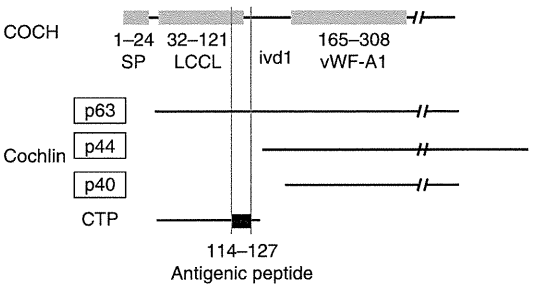

Figure 1. Representation of the antigenic peptide location, and the COCH gene, cochlin, and CTP. The top line denotes the deduced amino acid sequence of human COCH, showing the positions of the signal peptide (SP), Limulus factor C, cochlin, the late gestation lung protein Lgl1 domain (LCCL), intervening domain 1 (ivd1), and von Willebrand factor type A-like domain 1 (vWF-A1). The middle lines depict the cochlin isoforms p63s, p44s, and p40s that are expressed in inner ear tissue. The bottom line depicts the cochlin-tomoprotein (CTP) isoform expressed in the perilymph. The black bar indicates the location of the antigenic peptide and vertical lines represent the alignment of the antigenic peptide and cochlin isoforms. The numbers indicate the corresponding amino acid sequence of human cochlin.

were heated to 98°C for 5 min and then loaded into each lane of the gel. Electrophoresis was performed on 15% polyacrylamide gels (PAG mini Daiichi, Daiichi Pure Chemicals, Japan) in running buffer (25 mM Tris, 192 mM glycine, 1 g/l SDS, pH 8.3) at 20 mA for 2 h. The separated proteins were electrophoretically transferred onto a PVDF membrane (Immobilon-PSQ, Millipore, USA) using an Atto HorizBlot semi-dry transfer unit with a discontinuous buffer system, as recommended by the manufacturer (ATTO, Japan). Nonspecific binding was blocked by incubating the membranes overnight at 4°C in 5% skimmed milk and 0.2% polyoxyethylene sorbitan (Tween-20) dissolved in PBS. Membranes were then incubated in PBS containing 1% skimmed milk and 0.1% Tween-20 for 2 h at room temperature with the primary anti-LCCL-C Ab diluted at 1:2000. After washing in 0.05% Tween-20 in PBS, membranes were incubated for 1 h at room temperature with horseradish peroxidase-labeled goat anti-rabbit IgG (P0448, Dako, Denmark) diluted at 1:5000 in the same buffer used for the primary antibody reaction. The membranes were washed again and the reaction was developed with a chemiluminescence reaction kit (ECL Advance, GE Healthcare, England). The protein expression level of each isoform was determined with a densitometer LAS-3000 (Fuji Film, Japan), and the relative amount in each lane was calculated based on the p63 signal on DAB12 and the CTP signal on DAB24, respectively.

Real-time PCR

RNA preparation. Inner ear tissue was stored in RNAlater reagent (QIAGEN Inc., Mississauga, ON, Canada) at –80°C until RNA extraction. For the extraction of RNA, tissue was homogenized using 1.5 ml pellet pestles with Matching Microtubes (Kimble-Kontes, Vineland, NJ, USA) and QIAshredder spin columns (QIAGEN). Total RNA was extracted using an Ambion mirVana™miRNA Isolation Kit (Applied Biosystems, Foster City, CA, USA) following the manufacturer's protocol. The RNA concentration was determined by measuring absorbance at 260 nm with a spectrophotometer UV-1800 (Shimadzu, Kyoto, Japan), and the RNA concentration was normalized to 50 ng/μl.

Reverse transcription. Total RNAs from the membranous labyrinth were reverse-transcribed using a TaKaRa PCR Kit (AMV) Ver3.0 (Takara bio, Ohtsu, Shiga, Japan) with an oligo-dT-adapter primer for 30 min at 50°C, 5 min at 95°C, and 5 min at 5°C using a thermal cycler GeneAmp® PCR System 9700 (Applied Biosystems).

Real-time PCR assay validation. We conducted a preliminary study to validate the detection method, and verified the amplification efficiencies of COCH and the housekeeping gene GAPDH (glyceraldehyde-3-phosphate dehydrogenase) using RNA from the rat inner ear. The differences in the threshold cycle (ΔC_T) between COCH and GAPDH at serial dilutions of cDNA samples (×4, ×20, ×100, and ×500) were evaluated.

Real-time PCR assay. All the real-time PCR samples were set up in Fast96Well optical plates using 1 μl of cDNA. The reaction mixture was prepared using COCH primers (TaqMan Gene Expression Assays: Assay ID; Hs00187937_m1 Gene Symbol; hCG40905 Applied Biosystems). Since no TaqMan Gene Expression Assay targeting N terminus COCH mRNA was available, we selected a probe covering exon 8–9, which encodes the N-terminal portion of p40. Then 10 μl of 2× TaqManUniversal PCR Master Mix 10, 1 μl of 20× Primer&Probe Mixture, and 8 μl of RNA-free water were added to a final volume of 20 μl per reaction. GAPDH was used as a housekeeping gene. Then 10 μl of 2× TaqManUniversal PCR Master Mix (Applied Biosystems), 0.9 μl of 10 μM Forward and Reverse Primers, 0.5 μl of 5 μM TaqManProbe, and 6.7 μl of RNA-free water were added to a final volume of 20 μl per reaction.

All the samples were tested in triplicate. The real-time PCR program consisted of incubation at 50°C for 2 min, and 95°C for 10 min, 40 cycles at 95°C for 15 s, and 60°C for 1 min using the 7500 Real-Time PCR System (Applied Biosystems).

Data were evaluated using the $\Delta\Delta C_T$ method [14,15]. The method of Livak and Schmittgen [15] and the reference ΔC_T values obtained from the biological control GAPDH were applied for calculation of $\Delta\Delta C_T$ and the relative quantity values, respectively.

Results

Western blot analysis of cochlin isoform expression in the rat perilymph

The perilymph samples of eight ears (DAB12 and 18) and four ears (DAB 24, 30, and 70) were mixed and 0.5 μl of each sample was loaded into one lane. Using anti-LCCL-C Ab, immunoreactive proteins of 63 kDa and 16 kDa (CTP) were detected (Figure 2A). The level of protein expression for each was measured with a densitometer (LAS-3000; Fuji Film, Japan), and the relative amount of each band was calculated relative to the expression of p63 on DAB12, with the CTP on DAB18 taken as 100. Analysis was performed in triplicate and the data are presented as the mean ± standard

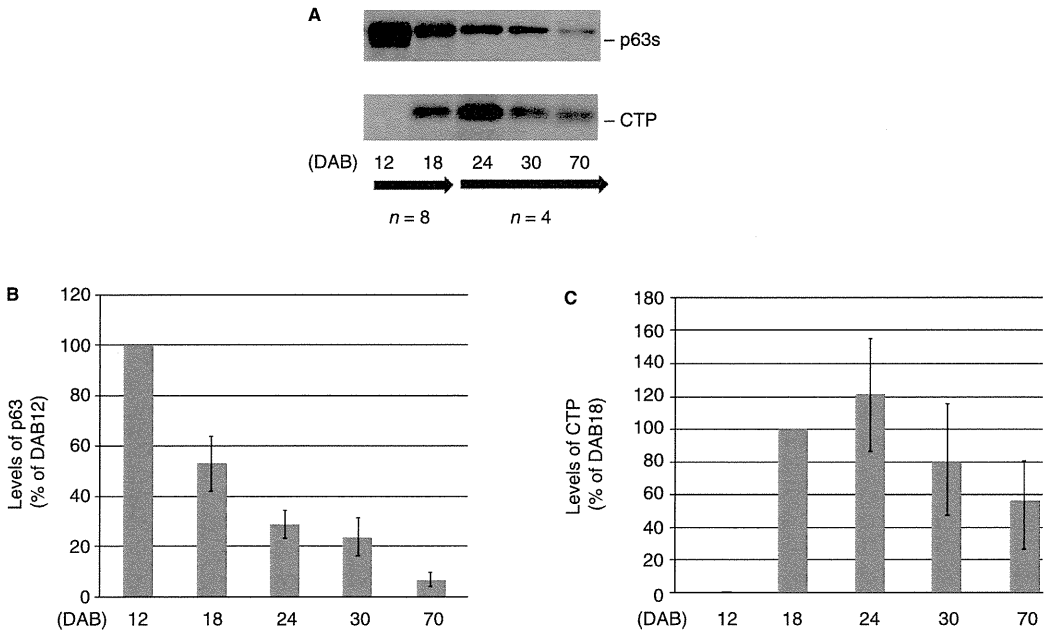

Figure 2. (A) Western blot analysis of perilymph proteins from the rat. Wistar rats on DAB 12 and 18 (n = 8 ears for each group) as well as DAB, 24, 30, and 70 (n = 4 ears for each group) were used for Western blot analysis of the perilymph. The samples from these ears were mixed for each DAB group. A representative Western blot is shown. The anti-LCCL-C antibody detected immunoreactive proteins of 63 kDa and 16 kDa (cochlin-tomoprotein, CTP). (B and C) The protein expression level of each of the isoforms in the perilymph: p63 (B) and CTP (C). The protein expression level of each isoform in the perilymph was measured by an LAS-3000 densitometer (Fuji Film, Japan), and the relative amount of each isoform was calculated relative to the expression of p63 on DAB12, with CTP on DAB18 taken as 100. Analysis was performed in triplicate and the data are presented as the mean ± standard error.

error. On DAB12, p63 expression was the highest among the perilymph samples tested and it gradually decreased to 52.8 ± 10.9% by DAB18, 28.7 ± 5.5% on DAB24, 23.7 ± 7.3% on DAB30, and then 6.7 ± 2.9% on DAB70. On the other hand, CTP expression was not detected on DAB12, detected on DAB18, and reached a peak of 121.4 ± 33.6% on DAB24. Then it gradually subsided to 80.3 ± 35.3% on DAB 30 and 56.7 ± 24.2% on DAB 70 (Figure 2B, C).

Real-time PCR assay validation

The threshold cycle (ΔC_T) difference between COCH and GAPDH in a serial dilution of cDNA samples (×4, ×20, ×100, and ×500) gave a linear slope of 0.0185, indicating that these genes have proportional expression efficiencies (Figure 3). It was appropriate to use the $\Delta\Delta C_T$ method since the slope of the standard curves of the COCH was <0.1.

Real-time PCR assay

The inner ear tissue of 20 ears (DAB 3, 6) or 10 ears (DAB 9, 12, 15, 24, 36, 70) was mixed and analyzed using real-time PCR assay. Comparative C_T ($\Delta\Delta C_T$) analysis was performed to evaluate the fold changes in mRNA expression. Analysis was performed in triplicate and the data are presented as the mean ± standard error. As shown in Figure 4, COCH mRNA was detected on DAB3, and continued to increase, reaching a maximum of 56.36 ± 0.84-fold on DAB15. Then it began to decrease gradually, and it was 10.73 ± 2.83-fold on DAB70.

Discussion

Cochlin, which is encoded by *COCH*, is a secreted protein for which the function is not completely understood, but it is believed to have a role in the formation and/or maintenance of the extracellular matrix (ECM) in the inner ear [1,16]. Cochlin appears to have numerous heterogeneous isoforms that are caused partly by N-glycosylation and proteolytic cleavage, and potentially also by alternative splicing [9,10,13,17]. Previous 2D gel investigation identified a full-length isoform, as well as smaller isoforms with truncations of the N terminus. The molecular weight values of the predominant isoforms were 44 and 40 kDa [10,12].

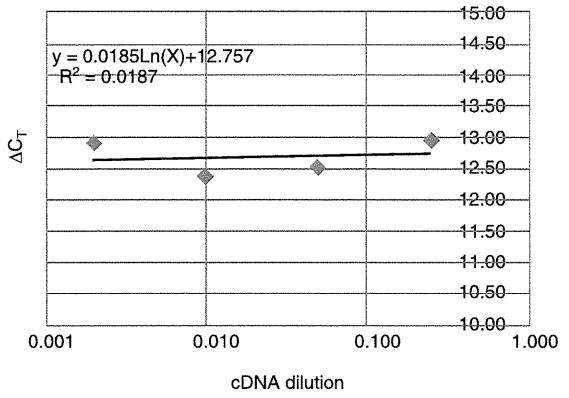

Figure 3. Real-time PCR assay validation. The differences in threshold cycle (ΔC_T) between COCH and GAPDH at serial dilution of cDNA samples (×4, ×20, ×100, and ×500) gave a lineal slope of 0.0185, indicating that both genes have proportional expression efficiencies.

Isoform-specific antibodies further identified the short truncated isoform CTP in the perilymph [10], and this isoform contains the N-terminal LCCL domain devoid of the C-terminal vWFA domain. The molecular weight of CTP is different in different species, e.g. rat (11–17 kDa), human (16 kDa), and bovine (18–23 kDa) [13].

The importance of cochlin has been shown in a variety of pathological conditions, such as DFNA9, autoimmune hearing loss, glaucoma, and others. One of the keys to understanding the pathogenetic mechanisms in these conditions is the analysis of the isoform expression patterns. Chance et al. [12] identified certain proteins and protein networks associated with cochlear pathogenesis in the Ames Waltzer (*av*)

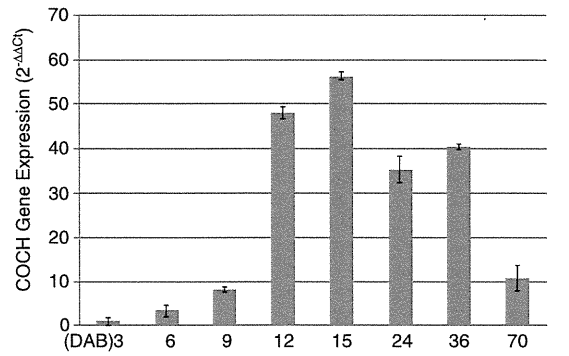

Figure 4. Real-time PCR assay of COCH gene expression in the developing inner ear tissue. The inner ear tissue of 20 ears (DAB 3, 6) or 10 ears (DAB 9, 12, 15, 24, 36, 70) was mixed and analyzed using real-time PCR assay. Comparative C_T ($\Delta\Delta C_T$) analysis was performed to evaluate the fold changes in mRNA expression. Analysis was performed in triplicate and the data are presented as the mean ± standard error.

mouse, a model for deafness in Usher syndrome 1F (USH1F). Sequence analysis by mass spectrometry showed that, in the *av* cochlea, a set of full-length cochlin isoforms was up-regulated, while the isoforms lacking the N-terminal FCH/LCCL domain were down-regulated. The potential effects that are conveyed by this molecular phenotype are currently unknown, but the observed change is counter to what has been reported in normal development. Our previous data indicated that the abundance of the full-length isoform p63s decreases relative to the abundance of the N-terminally truncated form p44s and p40s as a function of age in the rat, with the full-length isoform predominant on DAB24 but decreased relative to the truncated form on DAB70 [11,12].

In the present study, contrary to expectations, Western blot analysis showed that the expression of p63s in the perilymph was the highest on DAB12 and decreased gradually as the cochlea developed. On the other hand, CTP expression was lowest on DAB12 and increased gradually to DAB24. In our previous study of cochlin isoform expression analysis in inner ear tissue [11], p63s was below the detection limit on DAB13, but its expression gradually increased up to DAB24. On DAB70, p63s expression was lower than on DAB24. The N-terminally truncated forms, p44s and P40s, were not detected at DAB13 and were only weakly expressed from DAB17 to DAB70, although the expression did gradually increase up to DAB70 [11]. Notably, this change in p63 expression in the inner ear tissue is counter to what was found in the perilymph. p63 may be secreted into the perilymph in the early stage of postnatal inner ear development and then gradually come to be expressed in the inner ear tissue. The real-time PCR data on COCH expression confirmed the gene expression in the early stages, even though the expression level was minimal compared with that of DAB 12–24. The dynamic changes in the expression of the cochlin isoforms in the postnatal inner ear development suggest that cochlin plays an important role in the development and maturation process of the inner ear.

Perilymph is an important fluid not only for the delivery of the mechanical vibrations to hair cells, but also in the homeostatic regulation of certain ionic components, proteins, and other molecules, and it also provides a crucial microenvironment for labyrinthine cells. In our preliminary investigation, it was possible to microscopically identify the perilymphatic space as early as DAB12, and perilymph by itself could be collected without any other tissue contamination. Human, bovine, and rat perilymph contain two cochlin isoforms, the full-length isoform p63 and the short truncated isoform CTP [10,13]. The origin of these cochlin isoforms has been attributed to a variety of mechanisms, including proteolysis of

peptide bonds, chemical modifications such as glycosylation, phosphorylation and/or deamination, and multiple transcripts [9,17–19]. CTP may be formed by post-translational cleavage from full-length cochlin or directly encoded by a unique COCH gene splice variant [13]. Of the 13 DFNA9 mutations now reported for the COCH gene, 10 affect the residues of the LCCL domain. Yao et al. recently showed that full-length cochlin with mutations in this domain is cytotoxic when it is introduced into the perilymphatic space in vivo [20]. This study also suggests that mutant CTP in the perilymph may be harmful to inner ear function.

An adequate elucidation of the formation and processing of the cochlin isoforms, including the isoforms expressed in the perilymph, would provide insight into cochlin in the developing ear and mechanistic clues to how it is that mutations in the COCH gene damage the inner ear and other organs.

Declaration of interest: The authors report no conflicts of interest. The authors alone are responsible for the content and writing of the paper.

References

[1] Robertson NG, Lu L, Heller S, Merchant SN, Eavey RD, McKenna M, et al. Mutations in a novel cochlear gene cause DFNA9, a human nonsyndromic sensorineural deafness with vestibular dysfunction. Nat Genet 1998;20:299–303.

[2] de Kok YJ, Bom SJ, Brunt TM, Kemperman MH, van Beusekom E, van der Velde-Visser SD, et al. A Pro51Ser mutation in the COCH gene is associated with late onset autosomal dominant progressive sensorineural hearing loss with vestibular defects. Hum Mol Genet 1999;8:361–6.

[3] Usami S, Takahashi K, Yuge I, Ohtsuka A, Namba A, Abe S, et al. Mutations in the *COCH* gene are a frequent cause of autosomal dominant progressive cochleo-vestibular dysfunction, but not of Meniere's disease. Eur J Hum Genet 2003;11:744–8.

[4] Jones SM, Robertson NG, Given S, Giersch AB, Liberman MC, Morton CC. Hearing and vestibular deficits in the Coch(-/-) null mouse model: comparison to the Coch (G88E/G88E) mouse and to DFNA9 hearing and balance disorder. Hear Res 2011;272:42–8.

[5] Hildebrand MS, Gandolfo L, Shearer AE, Webster JA, Jensen M, Kimberling WJ, et al. A novel mutation in COCH – implications for genotype-phenotype correlations in DFNA9 hearing loss. Laryngoscope 2010;120:2489–93.

[6] Bom SJ, Kemperman MH, De Kok YJ, Huygen PL, Verhagen WI, Cremers FP, et al. Progressive cochleovestibular impairment caused by a point mutation in the COCH gene at DFNA9. Laryngoscope 1999;109:1525–30.

[7] Baek MJ, Park HM, Johnson JM, Altuntas CZ, Jane-Wit D, Jaini R, et al. Increased frequencies of cochlin-specific T cells in patients with autoimmune sensorineural hearing loss. J Immunol 2006;177:4203–10.

[8] Bhattacharya SK, Rockwood EJ, Smith SD, Bonilha VL, Crabb JS, Kuchtey RW, et al. Proteomics reveal Cochlin deposits associated with glaucomatous trabecular meshwork. J Biol Chem 2005;280:6080–4.

[9] Ikezono T, Omori A, Ichinose S, Pawankar R, Watanabe A, Yagi T. Identification of the protein product of the Coch gene (hereditary deafness gene) as the major component of bovine inner ear protein. Biochim Biophys Acta 2001;1535: 258–65.

[10] Ikezono T, Shindo S, Li L, Omori A, Ichinose S, Watanabe A, et al. Identification of a novel Cochlin isoform in the perilymph: insights to Cochlin function and the pathogenesis of DFNA9. Biochem Biophys Res Commun 2004; 314:440–6.

[11] Shindo S, Ikezono T, Ishizaki M, Sekiguchi S, Mizuta K, Li L, et al. Spatiotemporal expression of cochlin in the inner ear of rats during postnatal development. Neurosci Lett 2008;444:148–52.

[12] Chance MR, Chang J, Liu S, Gokulrangan G, Chen DH, Lindsay A, et al. Proteomics, bioinformatics and targeted gene expression analysis reveals up-regulation of cochlin and identifies other potential biomarkers in the mouse model for deafness in Usher syndrome type 1F. Hum Mol Genet 2010; 19:1515–27.

[13] Sekine K, Ikezono T, Matsumura T, Shindo S, Watanabe A, Li L, et al. Expression of cochlin mRNA splice variants in the inner ear. Audiol Neurootol 2010;15:88–96.

[14] Schmittgen TD, Livak KJ. Analyzing real-time PCR data by the comparative C(T) method. Nat Protoc 2008;3: 1101–8.

[15] Livak KJ, Schmittgen TD. Analysis of relative gene expression data using real-time quantitative PCR and the 2(-Delta Delta C(T)) Method. Methods 2001;25:402–8.

[16] Robertson NG, Cremers CW, Huygen PL, Ikezono T, Krastins B, Kremer H, et al. Cochlin immunostaining of inner ear pathologic deposits and proteomic analysis in DFNA9 deafness and vestibular dysfunction. Hum Mol Genet 2006;15:1071–85.

[17] Kommareddi PK, Nair TS, Raphael Y, Telian SA, Kim AH, Arts HA, et al. Cochlin isoforms and their interaction with CTL2 (SLC44A2) in the inner ear. J Assoc Res Otolaryngol 2007;8:435–46.

[18] Robertson NG, Skvorak AB, Yin Y, Weremowicz S, Johnson KR, Kovatch KA, et al. Mapping and characterization of a novel cochlear gene in human and in mouse: a positional candidate gene for a deafness disorder, DFNA9. Genomics 1997;46:345–54.

[19] Robertson NG, Hamaker SA, Patriub V, Aster JC, Morton CC. Subcellular localisation, secretion, and post-translational processing of normal cochlin, and of mutants causing the sensorineural deafness and vestibular disorder, DFNA9. J Med Genet 2003;40:479–86.

[20] Yao J, Py BF, Zhu H, Bao J, Yuan J. Role of protein misfolding in DFNA9 hearing loss. J Biol Chem 2010;285: 14909–19.